Adiabatic Microring Modulators

Aleksandr Biberman, Erman Timurdogan, and Michael R. Watts
Research Laboratory of Electronics, Massachusetts Institute of Technology, 77 Massachusetts Avenue, Cambridge, Massachusetts 02139, USA
biberman@mit.edu, mwatts@mit.edu

William A. Zortman and Douglas C. Trotter
Sandia National Laboratories, P. O. Box 5800, Albuquerque, New Mexico 87185, USA

Abstract: In this work, we demonstrate and experimentally characterize adiabatic microring modulators, the smallest (4-μm-diameter) microring modulators shown to date, yielding 6.92-THz uncorrupted free spectral ranges. We demonstrate and quantify operation up to 12.5-Gb/s data rates.

OCIS codes: (250.3140) Integrated optoelectronic circuits; (250.4110) Modulators; (130.0250) Optoelectronics.

1. Introduction

Compact, high-speed, low-power, and CMOS-compatible silicon photonic devices and systems are being widely considered for achieving aggressive performance goals in future computation and communication systems [1,2]. Silicon microring modulators, first demonstrated by Q. Xu *et al.* [3], have been primarily considered for these applications because they are capable of enabling WDM systems supporting many wavelength channels. Depletion-based microdisk modulators have improved on these early designs, enabling 3-fJ/bit operation [4], with a device that occupies less than one-tenth the area of traditional microring modulators, and maintains entirely-interior electrical contacts. However, one major limitation of microdisk resonators is that they support higher-order spatial modes that corrupt the free spectral range (FSR) with undesired resonances. In this work, we present the design and first quantitative results of a microring modulator based on an adiabatic microring resonator, which incorporates all of the benefits offered by modulators based on microdisk resonators, without corrupting the FSR [5,6].

The adiabatic microring modulator consists of a single-mode coupling region and multimode contact region (Fig. 1a). In the coupling region, the microring waveguide has a width of 460 nm, and the bus waveguide has a width of 320 nm, both kept narrow to ensure single-mode operation. The coupling gap was then chosen to be 360 nm, and designed to ensure critical coupling on resonance. The microring waveguide is adiabatically widened with a half ellipse inner radius to enable electrical contact where there is essentially no optical field. At the widest point, the microring waveguide reaches a width of 760 nm, and the microring is clearly multimode. However, the single-mode coupling region and adiabatic transition to the multimode contact region ensure that only the fundamental radial mode is excited (Fig. 1b). The structures are first tested passively (Fig. 1c); as also predicted by simulation [5], the adiabatic microring achieves a wide, 6.92-THz FSR, uncorrupted by higher-order spatial modes. These devices were fabricated on a 240-nm-thick silicon-on-insulator (SOI) platform, with a 1-μm buried oxide (BOX) layer, using 248-nm deep ultraviolet (DUV) lithography. All of these modulators (Fig. 2a,b) incorporate 400-nm-diameter tungsten contacts. The anode (cathode) contact connects to the 10^{20} P+ type (N+ type) doped silicon using titanium silicide at the interface, which then connects to the 2×10^{18} P type (N type) doped silicon. The P and N type doped silicon layers are each approximately 100-nm thick, which form depletion regions at their vertical junctions. The P+ type (N+ type) doped silicon is 100-nm (240-nm) thick to connect to the P type (N type) doped silicon on the top (bottom).

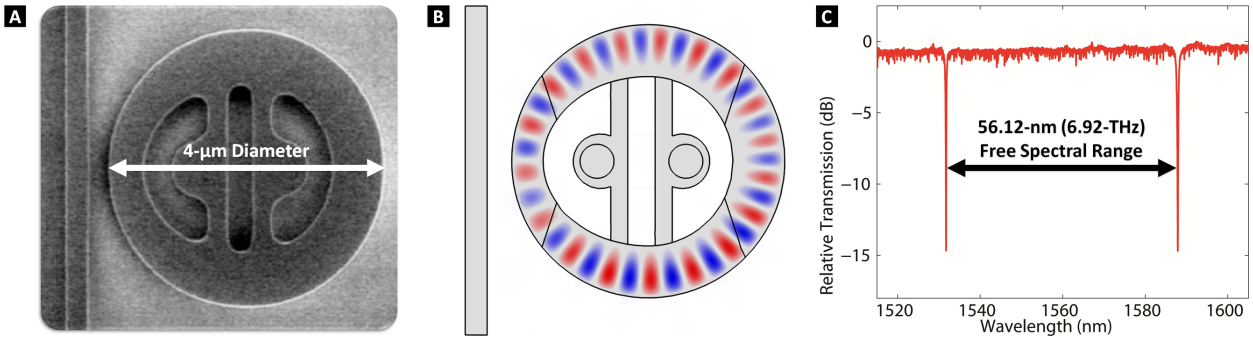

Fig. 1. (a) Top-view scanning-electron-microscope (SEM) image of the silicon adiabatic microring modulator, which comprises a 4-μm-diameter microring resonator. (b) 3D finite-difference time-domain (FDTD) simulation overlaying the schematic, showing that only the fundamental radial mode is excited. (c) Spectral response of this device, showing two consecutive resonances with an uncorrupted 56.12-nm (6.92-THz) free spectral range (FSR).

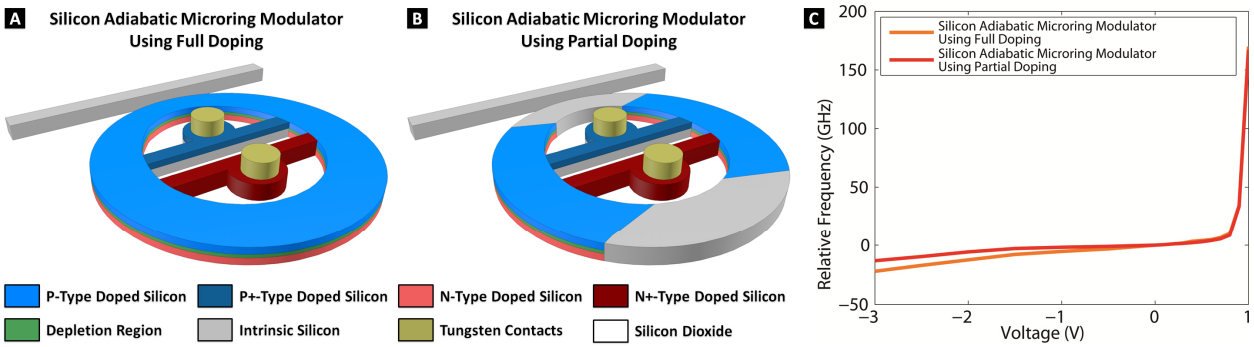

Fig. 2. Silicon adiabatic microring modulators, with (a) full and (b) partial doping configurations. (c) Experimentally-measured resonance frequency shifts, induced by varying applied DC voltages at the modulator diode junction, for both silicon photonic modulators.

2. Experimental Setup and Results of High-Speed Electro-Optic Performance Characterization

The experimental setup to characterize the silicon photonic modulators consists of a tunable laser source, which transmits a CW lightwave into the silicon chip using lensed fibers. Once on chip, the lightwave is then spectrally aligned to a resonance of the adiabatic microring resonator (1588 nm). This resonance is then spectrally shifted back and forth when we toggle an electrical bias, which toggles the depth of the depletion region through the vertical PN diode. The electrical bias is a non-return-to-zero (NRZ) on-off-keyed (OOK) signal, generated using a pattern generator (PG), encoded with a 2^{31}–1 pseudo-random bit sequence (PRBS). This signal is then amplified and offset to produce a 2.5-V_{PP} electrical signal with a –1-V voltage bias, with is transmitted into the chip using 50-Ω-terminated electrical probes. Because the modulators in this work employ the depletion-based configuration, which does not suffer from electrical carrier lifetime limitations, there is no need to supplement the driving signal with pre-emphasis.

Off chip, the high-speed optical signal then passes through an erbium-doped fiber amplifier (EDFA), a tunable grating filter (λ) with a 1-nm 3-dB bandwidth, and a variable optical attenuator (VOA). The signal is then received using a high-speed PIN photodiode and transimpedance amplifier (PIN-TIA) receiver followed by a limiting amplifier (LA), and is evaluated using a bit-error-rate (BER) tester (BERT). Both the PG and the BERT are synchronized to the same clock. Using a power tap, a digital communications analyzer (DCA) is used to examine the temporal response of the signal before the receiver. Polarization controllers (PCs) are also used throughout the setup, configured for TE operation. The total fiber-to-fiber insertion loss is about 17 dB for all of the devices; there is about –8-dBm (–19-dBm) average optical power ingressing into the modulator (EDFA), in every configuration. In the experimental setup comparing the performance of the silicon photonic modulators to a commercial lithium niobate Mach-Zehnder modulator, we replace the silicon chip with the commercial modulator. The lithium niobate modulator has a 35-GHz 3-dB bandwidth, and is driven with an AC-coupled 5.5-VPP electrical signal. For this modulator, there is also about –8-dBm average optical power ingressing into the modulator, and a VOA is used right after the modulator to ensure that –19-dBm average optical power is ingressing into the EDFA.

Resonance frequency shifts, induced by varying applied DC voltages at the modulator diode junction, show similar performance for both silicon photonic modulators (Fig. 2c). For data rates between 2.5 and 12.5 Gb/s (Fig. 3a,b), we record eye diagrams of the optical signals egressing from both silicon adiabatic modulators. For both devices, we see good noise performance up to 7.5 Gb/s. For the fully-doped device, we observe an increasing degradation of the optical signal above 7.5 Gb/s (Fig. 3a); at 12.5 Gb/s, the eye diagram becomes too distorted to distinguish the bits of the pattern. However, using the partially-doped device, we observe a dramatic improvement in the optical signal integrity (Fig. 3b). The partial doping enables operation at 12.5-Gb/s data rates and beyond. We also perform a similar characterization of the commercial lithium niobate Mach-Zehnder modulator (Fig. 3c), for the baseline back-to-back measurements. We perform BER measurements and power penalty characterizations for both silicon photonic modulators, and the commercial lithium niobate modulator, operating data rates up to 10 Gb/s. Here, the power penalty is the relative signal integrity of each silicon photonic modulator, compared to the commercial lithium niobate modulator (Fig. 4). For the silicon adiabatic microring modulator using full doping, we observe a moderate positive power penalty of 1.44 and 3.77 dB, at the data rate of 5 and 7.5 Gb/s, respectively. As we then modulate at 10 Gb/s, the signal degradation is so large for this device that it is no longer capable of achieving error-free operation. However, the silicon adiabatic microring modulator using partial doping achieves a moderate positive power penalty of 1.12, 2.05, and 2.20 dB, for 5, 7.5, and 10 Gb/s. This partially-doped version of the modulator outperforms the fully-doped modulator at every data rate, and is capable of achieving error-free operation at least up to 10 Gb/s. Lastly, we measure the dynamic extinction ratio and insertion loss for each modulator at every data rate up to 12.5 Gb/s (Fig. 4).

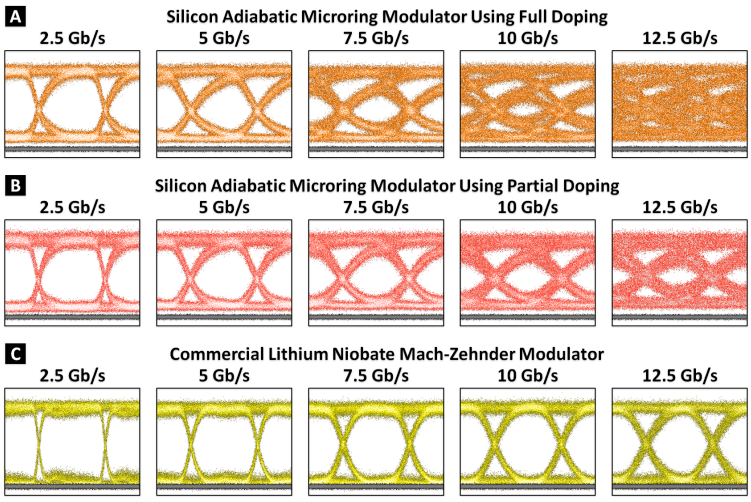

Fig. 3. Experimentally-measured optical eye diagrams egressing from the two silicon adiabatic microring modulators, with (a) full and (b) partial doping configurations, and (c) the commercial lithium niobate modulator, for data dates up to 12.5 Gb/s. The eye diagrams are overlaid with the true zero of each configuration.

Modulator Type	Data Rate	Extinction Ratio (dB)	Insertion Loss (dB)	Power Penalty (dB)
Silicon Adiabatic Microring Modulator Using Full Doping	2.5	8.52	0.70	–
	5	8.69	1.16	1.44
	7.5	7.93	1.43	3.77
	10	8.20	1.60	–
	12.5	7.73	1.66	–
Silicon Adiabatic Microring Modulator Using Partial Doping	2.5	9.03	1.86	–
	5	8.67	1.99	1.12
	7.5	8.15	2.59	2.05
	10	8.21	2.25	2.20
	12.5	7.34	2.59	–
Commercial Lithium Niobate Mach-Zehnder Modulator	2.5	14.24	4.00	–
	5	13.59	4.00	–
	7.5	12.67	4.00	–
	10	11.56	4.00	–
	12.5	11.49	4.00	–

Fig. 4. Table summarizing the experimentally-measured performance of both two silicon photonic modulators, and the commercial lithium niobate modulator, for data rates up to 12.5 Gb/s data rates. The measured power penalty of the adiabatic silicon microring modulators is in reference to the measured performance of the commercial lithium niobate modulator.

3. Conclusions

The silicon adiabatic microring modulator combines the best of all modulator designs, yielding an uncorrupted 56.12-nm (6.92-THz) FSR that can sustain over 100 wavelength channels in WDM systems. This compact, high-speed, and low-power modulator was also fabricated using standard CMOS-compatible wafer-scale photolithography, capable of dense integration with advanced electronics, and low-cost mass-volume production.

This work was supported in part by the Defense Advanced Research Projects Agency (DARPA) Microsystems Technology Office (MTO) Photonically Optimized Embedded Microprocessors (POEM) program, under the Silicon Photonic 3D-Integrated Reduced Energy Transmission (SPIRET) project, contract 6925995. Sandia National Laboratories is a multi-program laboratory managed and operated by Sandia Corporation, a wholly owned subsidiary of Lockheed Martin Corporation, for the U.S. Department of Energy's National Nuclear Security Administration under contract DE-AC04-94AL85000.

4. References

[1] D. A. B. Miller, "Device requirements for optical interconnects to silicon chips," *Proc. IEEE* **97,** 1166–1185 (2009).
[2] A. Biberman, "Silicon photonic revolution through advanced integration," *Future Fab Intl.* **42,** 25–28 (2012).
[3] Q. Xu, B. Schmidt, S. Pradhan, and M. Lipson, "Micrometre-scale silicon electro-optic modulator," *Nature* **435,** 325–327 (2005).
[4] M. R. Watts, W. A. Zortman, D. C. Trotter, R. W. Young, and A. L. Lentine, "Vertical junction silicon microdisk modulators and switches," *Opt. Express* **19,** 21989–22003 (2011).
[5] M. R. Watts, "Adiabatic microring resonators," *Opt. Lett.* **35,** 3231–3233 (2010).
[6] E. Timurdogan, M. Moresco, A. Biberman, J. Sun, W. A. Zortman, D. C. Trotter, and M. R. Watts, "Adiabatic resonant microring (ARM) modulator," Proc. Optical Interconnects Conference (OI Conference), TuC6 (2012).